



RESEARCH ARTICLE

Large CRISPR-Cas-induced deletions in the oxamniquine resistance locus of the human parasite *Schistosoma mansoni*

[version 1; peer review: 4 approved]

Geetha Sankaranarayanan*, Avril Coghlan*, Patrick Driguez ,
Magda E. Lotkowska, Mandy Sanders, Nancy Holroyd, Alan Tracey ,
Matthew Berriman , Gabriel Rinaldi 

Wellcome Sanger Institute, Hinxton, CB10 1SA, UK

* Equal contributors

V1 First published: 23 Jul 2020, 5:178
<https://doi.org/10.12688/wellcomeopenres.16031.1>
Latest published: 23 Jul 2020, 5:178
<https://doi.org/10.12688/wellcomeopenres.16031.1>

Abstract

Background. At least 250 million people worldwide suffer from schistosomiasis, caused by *Schistosoma* worms. Genome sequences for several *Schistosoma* species are available, including a high-quality annotated reference for *Schistosoma mansoni*. There is a pressing need to develop a reliable functional toolkit to translate these data into new biological insights and targets for intervention. CRISPR-Cas9 was recently demonstrated for the first time in *S. mansoni*, to produce somatic mutations in the *omega-1* ($\omega 1$) gene.

Methods. We employed CRISPR-Cas9 to introduce somatic mutations in a second gene, *SULT-OR*, a sulfotransferase expressed in the parasitic stages of *S. mansoni*, in which mutations confer resistance to the drug oxamniquine. A 262-bp PCR product spanning the region targeted by the gRNA against *SULT-OR* was amplified, and mutations identified in it by high-throughput sequencing.


Results. We found that 0.3-2.0% of aligned reads from CRISPR-Cas9-treated adult worms showed deletions spanning the predicted Cas9 cut site, compared to 0.1-0.2% for sporocysts, while deletions were extremely rare in eggs. The most common deletion observed in adults and sporocysts was a 34 bp-deletion directly upstream of the predicted cut site, but rarer deletions reaching as far as 102 bp upstream of the cut site were also detected. The CRISPR-Cas9-induced deletions, if homozygous, are predicted to cause resistance to oxamniquine by producing frameshifts, ablating *SULT-OR* transcription, or leading to mRNA degradation *via* the nonsense-mediated mRNA decay pathway. However, no *SULT-OR* knock down at the mRNA level was observed, presumably because the cells in which CRISPR-Cas9 did induce mutations represented a small fraction of all cells expressing *SULT-OR*.

Open Peer Review

Reviewer Status 

Invited Reviewers

	1	2	3	4
version 1 23 Jul 2020	 report	 report	 report	 report

1. **Phillip LoVerde** , University of Texas Health Science Center at San Antonio, San Antonio, USA
2. **Arnon Jurberg**, Oswaldo Cruz Foundation, Rio de Janeiro, Brazil
3. **Mattie Pawlowic** , University of Dundee, Dundee, UK
4. **Patrick Skelly** , Tufts University, North Grafton, USA

Any reports and responses or comments on the article can be found at the end of the article.

Conclusions. Further optimisation of CRISPR-Cas protocols for different developmental stages and particular cell types, including germline cells, will contribute to the generation of a homozygous knock-out in any gene of interest, and in particular the *SULT-OR* gene to derive an oxamniquine-resistant stable transgenic line.

Keywords

Schistosoma mansoni, Sulfotransferase, Transfection, Transgenesis, Genome editing, CRISPR-Cas9, Amplicon sequencing, CRISPResso



This article is included in the [Wellcome Sanger Institute gateway](#).

Corresponding author: Gabriel Rinaldi (gr10@sanger.ac.uk)

Author roles: **Sankaranarayanan G:** Formal Analysis, Investigation, Methodology, Validation, Writing – Review & Editing; **Coghlan A:** Data Curation, Formal Analysis, Investigation, Software, Validation, Visualization, Writing – Original Draft Preparation, Writing – Review & Editing; **Driguez P:** Formal Analysis, Investigation, Validation, Writing – Review & Editing; **Lotkowska ME:** Investigation, Writing – Review & Editing; **Sanders M:** Project Administration, Writing – Review & Editing; **Holroyd N:** Project Administration, Writing – Review & Editing; **Tracey A:** Data Curation, Software, Writing – Review & Editing; **Berriman M:** Conceptualization, Funding Acquisition, Resources, Supervision, Writing – Review & Editing; **Rinaldi G:** Conceptualization, Formal Analysis, Investigation, Methodology, Project Administration, Resources, Supervision, Validation, Visualization, Writing – Original Draft Preparation, Writing – Review & Editing

Competing interests: No competing interests were disclosed.

Grant information: This work was supported by the Wellcome Trust through a Strategic Award to MB [107475] and core funding to the Wellcome Sanger Institute [206194].

The funders had no role in study design, data collection and analysis, decision to publish, or preparation of the manuscript.

Copyright: © 2020 Sankaranarayanan G *et al.* This is an open access article distributed under the terms of the [Creative Commons Attribution License](#), which permits unrestricted use, distribution, and reproduction in any medium, provided the original work is properly cited.

How to cite this article: Sankaranarayanan G, Coghlan A, Driguez P *et al.* **Large CRISPR-Cas-induced deletions in the oxamniquine resistance locus of the human parasite *Schistosoma mansoni* [version 1; peer review: 4 approved]** Wellcome Open Research 2020, **5**:178 <https://doi.org/10.12688/wellcomeopenres.16031.1>

First published: 23 Jul 2020, **5**:178 <https://doi.org/10.12688/wellcomeopenres.16031.1>

Introduction

Schistosomiasis is a major neglected tropical disease (NTD) affecting more than 250 million people worldwide¹. *Schistosoma mansoni* and *S. japonicum* are the agents of hepato-intestinal schistosomiasis manifested by abdominal pain, liver inflammation and fibrosis that leads to portal hypertension. Infection with *S. haematobium*, agent of urogenital schistosomiasis, is associated with infertility, haematuria, kidney pathology and squamous cell carcinoma of the bladder. In addition, all forms of schistosomiasis are associated with systemic morbidities that include malnutrition, anaemia, physical and/or cognitive impairment and stunted development in children². Currently, praziquantel is the single effective drug to treat the infection, and is employed in mass drug administration programmes across endemic areas, which could eventually lead to drug resistance emerging³. Therefore, there is an urgent need for the development of novel drugs and vaccines⁴. Understanding the basic biology of schistosomes at the cellular and molecular levels is critical to identify exploitable vulnerabilities of the parasite. High-throughput datasets, including high quality reference genomes for the three main species of schistosomes⁵⁻⁷, have been generated. More recently, a thorough transcriptome analysis during the parasite's intra-mammalian development⁸, and the identification of different cell types by single-cell RNA sequencing of various life cycle stages^{9,10} represent significant steps towards deciphering cell fate and pathways involved in parasite development and host-parasite interactions.

In parallel to the generation of large-scale datasets, a functional genomics toolkit is needed to experimentally investigate hypotheses that emerge from these data, to confirm biological insights and validate targets for intervention. Recently, a large RNAi-based gene silencing screen, encompassing almost one third of *S. mansoni* protein-coding genes, revealed genes associated with parasite viability and potential targets for drug development¹¹. However, not every gene is susceptible to RNAi, the effect is transient and highly variable depending on the expression level, tissue localisation and half-life of the target mRNA and protein. In addition, off-target effects are common, in particular when long dsRNA molecules are used, and the gene silencing is typically not heritable unless an RNAi-based construct is employed as a transgene expressed in the germ line¹². Therefore, to truly examine gene function across the life-cycle, transgenesis-based approaches already available for model organisms^{13,14} need to be developed for *S. mansoni*, including protocols to create genetically-modified parasite strains with homozygous gene knock-outs, and site-specific gene mutations.

Promising progress with transgenesis and genome editing has been achieved. Retrovirus transduction of schistosome developmental stages, including eggs, has proved effective, and will likely be a key delivery system in the generation of stable transgenic lines¹⁵⁻¹⁸. Site-specific integration of transgenes and highly precise site-specific genome editing using CRISPR-Cas technology will be a key step¹⁹. CRISPR-Cas9 has recently been used to create a heritable gene knock-out line in the parasitic nematode *Strongyloides stercoralis*²⁰. In *S. mansoni*, the

technology has been used to produce mutations in the *omega-1* (*ω1*) gene in somatic cells of the egg²¹, and in a related parasitic flatworm, the liver fluke *Opisthorchis viverrini*, CRISPR-Cas9 mutations have been introduced into the granulysin gene in somatic cells of adult worms²². Somatic mutations in these two flatworms were associated with dramatic reductions in *ω1* and granulysin mRNA levels, respectively, and produced *in vitro* and *in vivo* phenotypic effects shedding new light on their functional roles and contributions to pathogenesis^{21,22}.

Whether different CRISPR-Cas protocols are needed to deliver site-specific mutations in *S. mansoni* genes expressed in other tissues or developmental stages remains to be determined. Likewise, the types of mutations to be expected and the degree of mRNA knock-down in different genes is not yet known. In the current study we have used CRISPR-Cas9 to introduce site-specific mutations in a second *S. mansoni* gene, to better understand how the CRISPR-Cas system works when applied to *S. mansoni*. We compared the efficiency of the approach in different developmental stages of the parasite: eggs, mother sporocysts (the first intra-snail stage) and adult worms. The mutations produced by CRISPR-Cas9, including their sizes and locations, were characterised. We chose the *SULT-OR* sulfotransferase (*Smp_089320*) gene as a target because recessive mutations in this gene, both induced in laboratory conditions and detected in field samples, confer resistance to the drug oxamniquine (OXA)^{23,24}. In addition, it is mostly expressed in the intra-mammalian stages of the life cycle (schistosomula and adults)²⁵ that would likely be the target of any new intervention strategy. Our findings provide insights that will help pave the way towards using CRISPR-Cas to achieve the generation of stable genetically-engineered schistosomes.

Methods

Ethics statement

The complete life cycle of *Schistosoma mansoni* NMRI (Puerto Rican) strain is maintained at the Wellcome Sanger Institute (WSI) by breeding and infecting susceptible *Biomphalaria glabrata* snails and mice. The mouse experimental infections and rest of regulated procedures were conducted under the Home Office Project Licence No. P77E8A062 held by GR. All protocols were revised and approved by the Animal Welfare and Ethical Review Body (AWERB) of the WSI. The AWERB is constituted as required by the UK Animals (Scientific Procedures) Act 1986 Amendment Regulations 2012.

Animal procedures

To obtain the parasite material described below, susceptible *Biomphalaria glabrata* snails and mice are routinely infected. In brief, snails exposed to 30 *S. mansoni* miracidia are maintained in aerated tanks in water and moved into dark cupboards at 28°C when they start shedding cercariae. For the mouse infections, cercariae are collected by placing ~50 infected snails in a 200ml glass beaker containing water and exposed to bright light for an hour. To quantify the cercariae, 12 5µL aliquots of cercarial water are sampled, mixed with Lugol (cat.# 62650, Sigma Aldrich), and the larvae counted under a dissecting microscope. Thereafter, the cercarial solution is

diluted to a final concentration of 500 cercariae/ml, and immediately used for percutaneous infection. Eight to 12 weeks old outbred HsdOla:TO female mice are infected with 250 *S. mansoni* cercariae for 40 minutes by percutaneous infection through the tail. Briefly, tubes containing 5.5 ml of conditioned water are pre-filled and placed onto a bespoke anaesthesia rig. The mice are anaesthetised in an induction box using 4% isoflurane (Vetflurane®); 1 l/min oxygen, and eye ointment used to prevent corneal damage. Under anaesthesia, the mice are carefully transferred onto individual holders on the rigs and their tails inserted into the test tubes. Nose cones are adjusted for each animal, and anaesthesia is maintained at 2% isoflurane; 1 l/min oxygen. In each test tube, 500 µL of a stock solution containing 500 cercariae/ml is added (i.e. 250 cercariae per mouse). After 40 minutes, animals are removed from the anaesthesia rigs, placed back into their cage and monitored until full recovery from the anaesthesia.

At 6 weeks post infection the mice are euthanised by intraperitoneal injection of 200 µl of 200 mg/ml pentobarbital (Dolethal®) supplemented with 100 U/ml heparin (cat.# H3393, Sigma Aldrich), adult worms recovered by portal perfusion (the portal vein is sectioned followed by intracardiac perfusion with phenol-red-free DMEM, cat.# 31053-044 ThermoFisher Scientific, containing 10 U/mL heparin), and whole livers collected.

The outbred HsdOla:TO female mice are commercially outsourced (Envigo, UK), housed in GM500 Individually Ventilated Cages or IsoCage N -Biocontainment Systems (Tecniplast) and maintained on individual air handling units at 19 to 23°C and 45–65% humidity. Animals are given access to food and water *ad libitum*, maintained on a 12-hour light/dark cycle, and housed in groups of no more than 5 adults per cage. Welfare assessments are carried out daily abnormal signs of behaviour or clinical signs of concern are reported. All personnel at the WSI performing welfare checks on animals are trained and assessed as competent by qualified named individuals.

Parasite material

Developmental stages of *S. mansoni* were collected and maintained as described²⁶. In brief, mixed-sex adult worms were collected by portal perfusion of experimentally-infected mice 6 weeks after infection (above), washed with 1x Phosphate-Buffered Saline (PBS, cat.# D8662), supplemented with 200 U/ml penicillin, 200 µg/ml streptomycin and 500 ng/ml amphotericin B (cat.# 15240062), and cultured in complete high-glucose DMEM (cat.# 11995065), 10% fetal bovine serum (FBS, cat.# 10500064), 200 U/ml penicillin, 200 µg/ml streptomycin and 500 ng/ml amphotericin B (cat.# 15240062) at 37°C, under 5% CO₂ in air. All media components were purchased from ThermoFisher Scientific. *S. mansoni* eggs were isolated from the livers of experimentally-infected mice removed after the portal perfusion²⁷. The livers were finely minced and digested overnight in the presence of 0.5% *Clostridium histolyticum* collagenase (cat.# C5138, Sigma Aldrich), followed by three washes with 1x PBS and filtered through 250 µm and 150 µm sieves. The

filtrate was passed through a Percoll-sucrose gradient (Percoll cat.# P1644, Sucrose cat.# 84097, Sigma Aldrich), and the resulting purified eggs washed in 1x PBS and cultured in complete DMEM medium at 37°C, under 5% CO₂ in air as described²⁸. Primary sporocysts were obtained by transferring miracidia hatched from freshly collected eggs into complete sporocyst medium (MEMSE-J, 10% Fetal Bovine Serum, 10mM HEPES, 100 U/ml penicillin, 100 µg/ml streptomycin) and cultured in a hypoxia chamber in a gas mixture of 1% O₂, 3% CO₂ and balance N₂, at 28°C²⁶.

CRISPR-Cas 9 ribonucleoprotein complex assembly

We explored the activity of a ‘two-piece’ guide RNA that included a (1) CRISPR RNA (crRNA) molecule of 20 nucleotides target-specific sequence, and (2) the conserved 67 nucleotide trans-activating crRNA (tracrRNA). The crRNA sequence 5’-ACAATCCAAGTTATCTCAGC-3’, spanning positions 19-38 from the first codon of exon 1 of *SULT-OR* (*Smp_089320*) and followed by the protospacer adjacent motif (PAM) TGG (Figure 1), was designed using the web-based tool CRISPR RGEN Tools ([Computational tools and libraries for RNA-guided endonucleases](#), RGENs). The crRNA, the fluorescently labelled tracrRNA (Alt-R® CRISPR-Cas9 tracrRNA, ATTO™ 550), and the recombinant *Streptococcus pyogenes* Cas9 nuclease containing a nuclear localization sequence (Alt-R® S.p. Cas9 Nuclease V3) were purchased from IDT. The CRISPR-Cas9 ribonucleoprotein complex (RNP) was assembled *in vitro* by combining the ‘two-piece’ gRNA with the Cas9 nuclease (163.7 kDa). Briefly, the ‘two-piece’ gRNA was generated by mixing equal volumes of 200 µM *SULT-OR* crRNA and 200 µM ATTO™ 550 tracrRNA in IDT buffer. The RNA oligos were annealed by incubating the mixture at 95°C for 5 min followed by a slow cooling to room temperature for at least 10 min. Thereafter, the RNP was assembled by combining 100 pmol Cas9 nuclease (stock concentration, 10 µg/µl = 61 µM) with 150 pmol ‘two-piece’ gRNA. The RNP was gently mixed avoiding pipetting, incubated at room temperature for 10 min and kept on ice. Immediately before the parasite transfection Opti-MEM media (cat.# 31985070, ThermoFisher Scientific) was added to the RNP to reach a final volume of 100 µl and kept on ice.

CRISPR-Cas9 transfection of schistosome developmental stages

The CRISPR-Cas9 RNP was delivered into *S. mansoni* mixed-sex adult worms, eggs and *in vitro*-transformed mother sporocysts by square-wave electroporation as previously described^{29,30} with minor modifications. Briefly, groups of ~16 male and female worms were transferred to a pre-cooled 4-mm electroporation cuvette (BTX), and washed 3 times by gravity with Opti-MEM medium with no FBS and no antibiotic/antimycotic mix. After the last wash, the worms were maintained in 50 µl of Opti-MEM medium and the RNP in 100 µl of Opti-MEM medium (above) was added to the cuvette containing the worms. The eggs isolated from the livers and cultured as described above were collected and washed in Opti-MEM medium (no FBS and no antibiotic/antimycotic mix) 3 times by centrifugation at 400 g for 5 min. After the last wash, the eggs were split into groups of ~10,000, resuspended

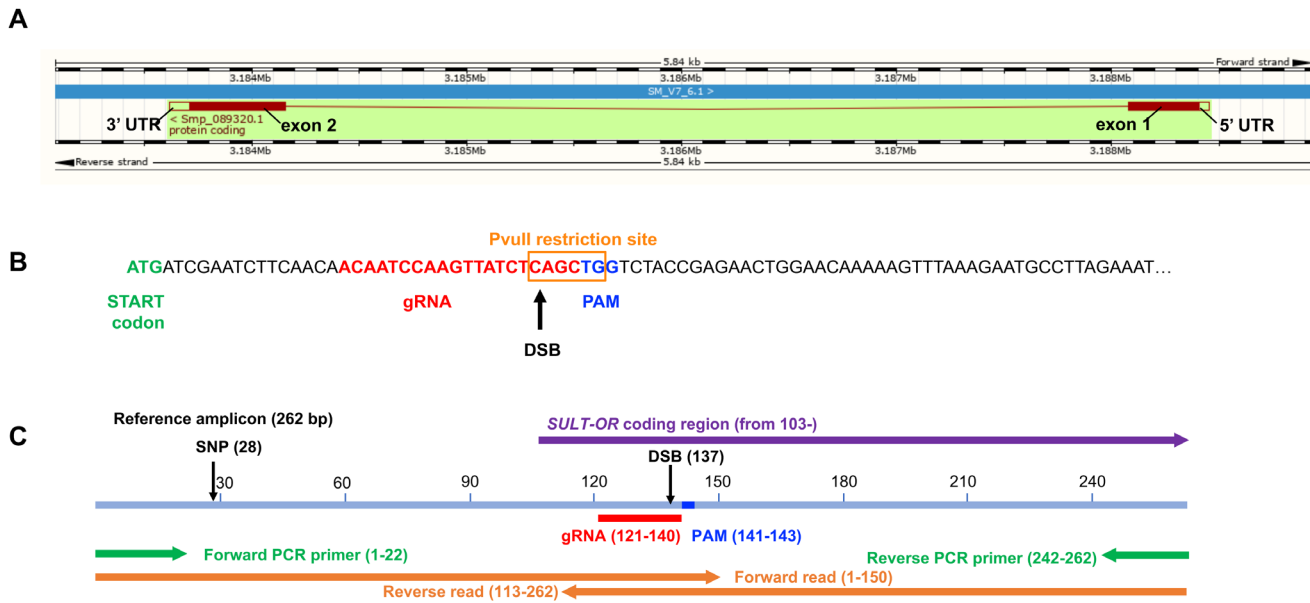


Figure 1. (A) Gene model of *SULT-OR* (*Smp_089320*), indicating the position of the two exons, one intron, and UTRs, spanning 4837 bp on the reverse strand of chromosome 6. Boxes filled in dark red represent the protein coding sequence. *Schistosoma mansoni* (PRJEA36577). Assembly: Smansoni_v7 (GCA_000237925.3). Region: Scaffold SM_V7_6:3,183,084-3,188,924. Adapted from WormBase ParaSite 14³¹. (B) Nucleotide sequence of the start of exon 1 indicating location and sequence of gRNA target site, predicted double-stranded break (DSB), protospacer adjacent motif (PAM), and the PvuII restriction site. (C) Reference PCR amplicon, showing the positions of the gRNA, PAM, DSB, forward and reverse PCR primers, and forward and reverse sequence reads, as well as a SNP site found in many sequence reads. The diagrams are drawn to scale.

in 100 μ l of Opti-MEM medium containing the RNP (above) plus 50 μ l of Opti-MEM to collect all the remaining eggs from the original tube, and transferred to a pre-cooled 4-mm electroporation cuvette (BTX). Three-day old *in vitro*-transformed sporocysts were collected and washed in Opti-MEM medium (no FBS and no antibiotic/antimycotic mix) 3 times by centrifugation at 400 g for 5 min. After the last wash, the sporocysts were split in groups of ~10,000, resuspended in 100 μ l of Opti-MEM medium containing the RNP (above) plus 50 μ l of Opti-MEM to collect all the remaining sporocysts from the original tube, and transferred to a pre-cooled 4-mm electroporation cuvette (BTX). The final electroporation volume for the schistosome worms, eggs and sporocysts was 150 μ l, i.e. the final concentration of the RNP complex in the cuvette was 1.67 μ M. The three developmental stages were subjected to the same electroporation conditions; square-wave, a single pulse of 125V for 20 msec in a BTX Gemini X2 electroporator (BTX). Immediately after electroporation, the schistosome worms and eggs were collected in pre-warmed complete DMEM medium, and the sporocysts in complete sporocysts medium and cultured as described above. Four hours after transfection, three male and female worms and a few thousand eggs and sporocysts were collected for confocal microscopy (below). Four days post-transfection the parasites were collected, washed in 1x PBS and processed for DNA and RNA isolation (below). In addition to the CRISPR-Cas9 experimental condition, i.e. parasites exposed to the CRISPR-Cas9 RNP complex, we included

three control groups subjected to the same electroporation protocol: (1) mock-treated group that included parasites exposed to no molecules, (2) parasites exposed to Cas9 nuclease only, and (3) parasites exposed to the 'two-piece' gRNA only. **Extended data Table S1** summarises the experimental conditions and biological replicates performed for each of the three tested developmental stages³².

DNA isolation and amplicon sequencing libraries

A conventional phenol:chloroform:isoamyl alcohol (25:24:1) protocol was employed to isolate DNA from RNP-transfected parasites and all control groups. Briefly, wet pellets of adult worms, eggs or mother sporocysts stored at -80°C were incubated overnight in the presence of 500 μ l genomic DNA lysis buffer (200 mM NaCl, 100 mM Tris-HCl pH 8.5, 50 mM EDTA pH 8, 0.5 % SDS) and 10 μ l of proteinase K (20 mg/ml, cat.# AM2546, Life Technologies) at 56°C with agitation (400 rpm). Thereafter, 5 μ l of 4 mg/ml of RNase A (cat.# 7973, Promega) was added to the lysate and incubated at 37°C for 10 min. One volume of phenol-chloroform-isoamyl alcohol (25:24:1) (cat.# p2069, Sigma-Aldrich) was added to the sample, mixed vigorously, incubated at room temperature for 5 min and centrifuged at 14,000 g at room temperature for 15 min. The aqueous top layer was transferred to a new tube, 1 volume (~200 μ l) of chloroform:isoamyl alcohol (24:1) (cat.# 327155000, Acros Organic) was added to the sample, mixed vigorously and centrifuged as above. The aqueous top layer was transferred

to a new tube and the DNA precipitated with 0.1 volume of 3 M sodium acetate, 3 volumes of 95%-100% ethanol, and 2 μ l of Glycoblu (cat.# AM9516, Thermo Fisher Scientific) overnight at -20°C. The DNA was recovered by centrifugation at 14,000 g at 4°C for 30 min, washed with 500 μ l of 70% ethanol, resuspended in pre-warmed nuclease-free water and quantified by Qubit fluorometer. For the indicated samples (**Extended data Table S1**³²) in order to enrich for *SULT-OR* mutant alleles, 20 ng of DNA was digested with 6 to 12 U of the restriction enzyme PvuII (PvuII-HF, cat.#R3151, NEB) overnight at 37°C.

For the amplicon library preparation, a 2-step PCR protocol was followed. During the first PCR, a 262 bp *SULT-OR*-specific amplicon spanning the predicted double-stranded breaking site (DBS) was generated using 10 ng template DNA (20 μ l of 0.5 ng/ μ l DNA preparation), 300 nM forward and reverse primers (**Extended data Table S2**³²), and 2x Kapa HiFi Master Mix (cat.# KK2602, Roche) in a 50 μ l PCR reaction performed in a Thermocycler (Eppendorf mastercycler X50s). The PCR protocol included an initial denaturation step at 95°C for 3 min, 18 cycles of denaturation step at 98°C for 20 sec, annealing step at 53°C for 15 sec, and extension step at 72°C for 40 sec, followed by a final extension step at 72°C for 5 min. Four PCR reactions per sample were run in parallel and the products were pooled at the end, i.e. a total of 40 ng of each sample DNA preparation was used to generate the amplicon. For sample DNA preparations that were digested with PvuII, two PCR reactions per sample were run in parallel and the products were pooled, i.e. a total of 20 ng of each of two PvuII-digested DNA preparations was used to generate the amplicon. The pooled PCR products for each sample were cleaned up using a column-based kit (cat.# D4014, Zymo DNA Clean and concentrator), eluted in 17 μ l of nuclease-free water; 2 μ l were used for quantification and the rest entirely used as template in the second PCR for Nextera Indexing (Nextera-XT Index kit -FC-131-1001). In a 50 μ l-reaction the concentrated DNA (15 μ l) was mixed with 10 μ l of the Nextera index mix (i5 + i7) and 2x Kapa HiFi Master Mix (cat.# KK2602, Roche). The PCR was performed in a Thermocycler (Eppendorf mastercycler X50s) with an initial denaturation step at 95°C for 3 min, 8 cycles of denaturation step at 98°C for 20 sec, annealing step at 55°C for 15 sec, and extension step at 72°C for 40 sec, followed by a final extension step at 72°C for 5 min. The PCR products were purified using a bead-based cleaner kit (cat.# A63880, AMPure XP, Beckman Coulter), eluted in 30 μ l of nuclease-free water and quantified using a high sensitivity DNA chip in a Bioanalyzer (2100 Bioanalyzer Instrument, Agilent Technologies). Equimolar amounts of each library were combined and 20–30% PhiX was added to the mix to introduce complexity into these low-diversity amplicon libraries.

Bioinformatic analysis

Amplicon libraries from the samples summarised in **Extended data Table S1** were sequenced on a MiSeq Illumina sequencing platform spiked with 20-30% PhiX to generate diversity³². If a sample had been multiplexed and run on several MiSeq lanes, the fastq files for that particular sample were merged.

Trimmomatic version 0.33³³ was used to discard low quality read-pairs where either read had average base quality < 23. To detect CRISPR-induced mutations, the software **CRISPResso** v1.0.13^{34,35} was employed using a window size of 500 bp (-w 500) with the reference amplicon according to *Smp_089320* in the *S. mansoni* V7 assembly from **WormBase ParaSite**, version 14.0 (August 2019)³¹. In most samples, the majority of reads had a G→A SNP at position 28 of the amplicon, presumably due to genetic variation in the population of *S. mansoni* NMRI strain maintained in our laboratory. Thus, although the *S. mansoni* V7 reference assembly has 'G' at this position, we used 'A' at this position in the 'reference amplicon' sequence given to CRISPResso. A window size of 500 bp was used to include the entire amplicon. CRISPResso was run with the -exclude_bp_from_left 30 and -exclude_bp_from_right 30 options in order to disregard the (21-22 bp) primer regions on each end of the amplicon, and the SNP at position 28, when indels and substitutions were being quantified and reads being classified as 'NHEJ' or 'unmodified' by CRISPResso.

Gene expression analysis for *SULT-OR* gene

Total RNA was extracted from adult worms, eggs or *in vitro* transformed sporocysts following a phenol:chloroform-based protocol. In brief, four days after transfection, parasites were collected from the culture, washed three times in 1x PBS complemented with antibiotic-antimycotic as described above for each of the three developmental stages, transferred to 1ml of Trizol, incubated at room temperature for ~10 min and stored at -80°C. The parasites in Trizol were mechanically-dissociated using a bead beater homogenizer (Fast Prep-24, MP Biomedicals) using two 20-second pulses at setting four for adult worms and *in vitro* transformed sporocysts, and two 20-second pulses at setting six, after three cycles of freezing-thawing, for eggs. Thereafter, one volume of chloroform was added to the samples, mixed vigorously, centrifuged at 14,000 g at room temperature for 15 min, and the aqueous top layer was carefully transferred to a clean tube. The total RNA was precipitated using an equal volume of 100% molecular biological grade ethanol. Residual DNA was removed by digestion with DNaseI (cat.# E1010, Zymo). RNA was cleaned and concentrated using Zymo RNA clean and concentrator columns, and eluted in 15 μ l of nuclease-free water. cDNA was synthesized from 65 -175 ng of total RNA using the iScript cDNA Synthesis Kit (cat.#1708891, Bio-Rad, Hercules, CA). Target-specific primers designed with the assistance of the free web-based **PrimerQuest® Tool** (IDT) are shown in **Extended data Table S2**, and the amplification efficiencies for each primer set were estimated to be 90–105% by titration analysis^{32,36}. Real time quantitative PCRs (qPCR) were performed in triplicate, in 96-well plates, following an initial denaturation step at 95°C for 3 min followed by 40 cycles of 30 sec at 95°C and 30 sec at 50 °C, and a final melting curve, in a StepOnePlus™ Real-Time PCR System (Applied Biosystems). Reactions run in 10 μ l included 300 nM of each target-specific primer, 1 μ l of cDNA, and Kapa Sybr FastqPCR Master Mix (cat.# KK4600, Roche). The relative quantification assay³⁷ was employed using both *S. mansoni* glyceraldehyde-3-phosphate dehydrogenase (*SmGAPDH*, *Smp_056970*) and *S. mansoni*

α -tubulin1 (*SmAT1*, *Smp_090120*) as reference genes. The target gene expression levels were normalised using the control group.

Confocal microscopy

Four hours after electroporation with fluorescently labelled RNP complex, transfected adult worms, eggs or mother sporocysts were collected from the culture, fixed and processed for confocal microscopy imaging. In brief, the parasites were collected and washed three times in 1x PBS complemented with antibiotic-antimycotic solution as described above; adult worms were washed by gravity, and eggs and sporocyst by centrifugation, 400 g for 5 min. After the final wash the parasites were fixed overnight in 4% methanol-free paraformaldehyde (cat.# 28906, Pierce™) diluted in 1x PBS at 4°C, washed three times in 1x PBS, resuspended in mounting media containing 4', 6'-diamidino-2-phenylindole (DAPI) for nuclear staining (cat.# 15596276, Fluoromount-G™ Mounting Medium, with DAPI, Invitrogen), and incubated overnight at 4°C. The parasites were mounted on microscope slides and images taken with a Leica SP8 confocal microscope using appropriate settings to capture DAPI and ATTO 550 fluorochromes. Manipulation of digital images was undertaken with the assistance of the LAS X software (Leica) and was limited to insertion of scale bars, adjustment of brightness and contrast, and cropping. The image enhancement algorithms were applied in a linear fashion across the entire image.

Accession numbers

The sequence data generated in this study are available at the European Nucleotide Archive (ENA) accession number [ERP121238](#). The accession number for each sample is shown in **Extended data Table S1**, columns P, Q³².

Statistical analysis

A paired one-sided Wilcoxon test (non-parametric) was used to analyse significant differences between percentages of aligned reads containing deletions (or insertions or substitutions) between CRISPR-Cas9-treated samples and respective matched controls. All Statistical analyses were performed using R, version 3.4.1.

Results

The *SULT-OR* gene belongs to a multi-copy locus on chromosome 6 of *S. mansoni*

The *SULT-OR* gene (*Smp_089320*) belongs to a multi-copy locus containing six other paralogous genes on chromosome 6 of the *S. mansoni* reference genome, version 7 ([WormBase ParaSite](#)), (**Extended data Figure S1A, B**³²). This locus in chromosome 6 has been correctly resolved with no evidence of repetitive regions that frequently appear 'collapsed' within assemblies (**Extended data Figure S1C**³²). The biological function of *SULT-OR* remains unknown, except that it converts the pro-drugs OXA and hycanthon to their active forms^{23,24}. It displays sulfotransferase activity *in vitro* on exogenous substrates²³, even though the protein shows a low level of sequence similarity to other sulfotransferases, and it is mostly expressed in the intra-mammalian stages of the life cycle

(schistosomula and adults, **Extended data Figure S2A**^{32,25}). Intriguingly, *SULT-OR* belongs to a gene family that has expanded in trematodes³⁸, suggesting it may play an important role in clade-specific biology. However, *ex vivo* *SULT-OR* RNAi experiments in adult male worms showed no evident phenotypic effects other than becoming resistant to OXA²³. Single-cell transcriptomic analysis of two-day-old schistosomula⁹, adult worms¹⁰, and *in vitro*-transformed mother sporocysts (unpublished) revealed *SULT-OR* mRNA is a marker of parenchymal cell clusters (**Extended data Table S3** and **Extended data Figure S2B**³²), while its top BLASTP hit in the planarian *Schmidtea mediterranea*, *dd_Smed_v6_9472_0*, is a marker of intestinal cells³⁹.

A specific gRNA to introduce mutations in exon 1 of *SULT-OR*

The *SULT-OR* gene comprises two coding exons separated by one intron, spans 4837 bp on the reverse strand of chromosome 6, and includes a short 46 bp 5'UTR (**Figure 1A**). A gRNA was designed to target residues 19 to 38 of the coding region of *SULT-OR* within exon 1, adjacent to a TGG protospacer adjacent motif (PAM) and with the predicted double strand break (DSB; i.e. the predicted Cas9 cut site) 3 bp upstream of the PAM (**Figure 1B**). Importantly, the sequences homologous to this gRNA's target region are relatively diverged in the paralogous genes on chromosome 6, with many mismatches within the seed region (10-12 bp at its 5' end) (**Extended data Figure S3A**³²). It has been shown that mismatches in the gRNA 'core' sequence located between 4 to 7 nucleotides upstream of the PAM abolishes off target cleavages^{19,40}; hence, our gRNA is expected to be specific to *SULT-OR*.

CRISPR-Cas9 machinery successfully delivered into schistosome developmental stages

To investigate whether the CRISPR-Cas9 machinery, i.e. RNP (ribonucleoprotein) complex containing the Cas9 nuclease and *SULT-OR*-specific gRNA, was successfully delivered into adult worms, sporocysts and eggs, we used fluorescently labelled RNP. Parasites were collected from culture four hours after transfection and fixed for confocal microscopy. The images revealed that the RNP complex entered cells of adult worms, sporocysts and eggs (**Figure 2**). Even though the parasites were thoroughly washed before fixation, a strong signal outside the tegument was evident, in particular in adult worms, suggesting RNP complex molecules unspecifically bound to the surface of the parasites (**Figure 2A** and **Movie 1**⁴¹). However, in addition to the signal in the surface of the parasite, the confocal optical sections revealed fluorescently-labelled cells within the body of both male and female worms (**Figure 2B**, **Extended data Figure S4A-C**³², **Movies 2** and **3**⁴¹). Interestingly, the majority of these successfully transfected cells were located around the intestine (**Figures 2B-D** and **Movie 1**⁴¹). The relatively higher concentration of the RNP complex surrounding the adult gut may have resulted from worms swallowing Cas9-gRNA molecules in the suspension before the electroporation step was carried out. The fluorescent signal in sporocysts was evenly distributed within the organism

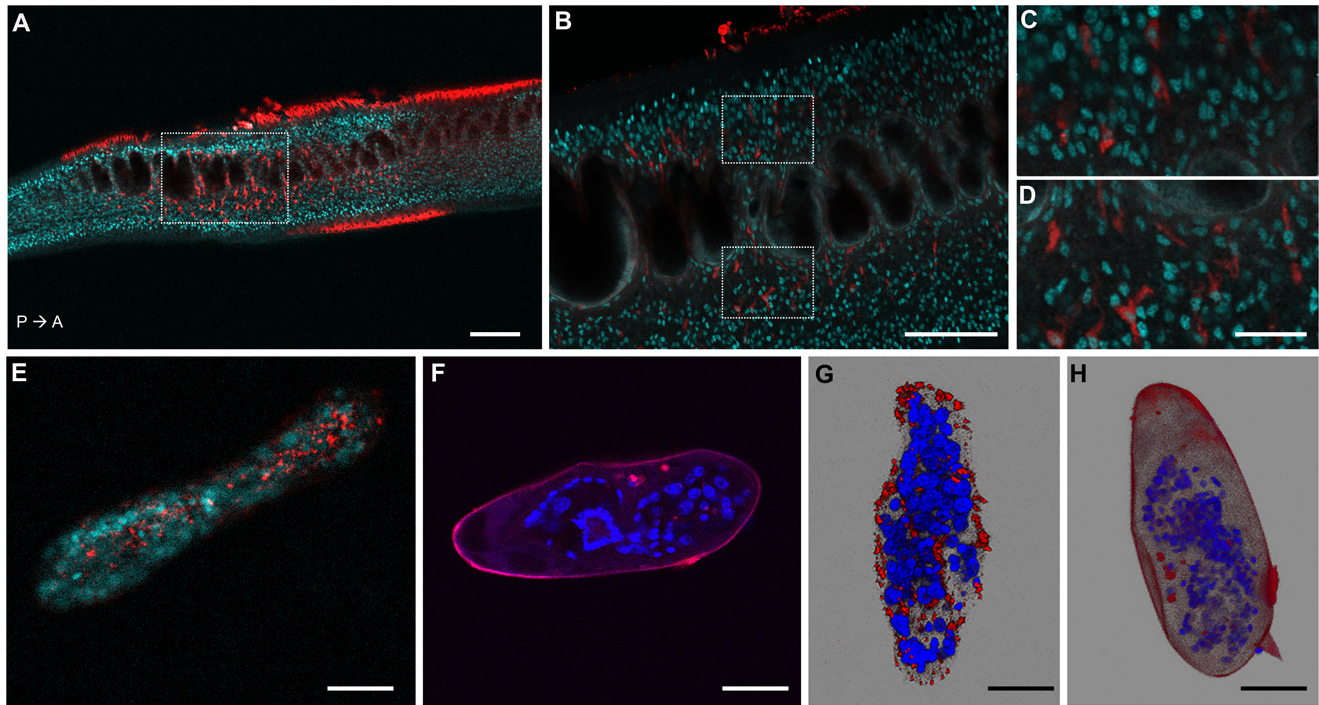


Figure 2. Confocal microscopy images of *S. mansoni* parasites transfected with fluorescently labelled Cas9-gRNA (ATTO™ 550 signal in red), fixed and DAPI-stained (DAPI signal in aqua blue or blue). **(A)** Confocal optical section of a male adult worm. P→A: indicates the posterior anterior axis. Scale bar: 100 μ m. **(B)** Magnified squared-area in **(A)**. Scale bar: 50 μ m. **(C, D)** Magnified top and bottom squared-areas in **(B)**, respectively. Scale bar: 10 μ m. **(E, F)** Confocal optical sections of a sporocyst and an egg, respectively. **(G, H)** Maximum intensity projection of z-stack images of a sporocyst and an egg, respectively. Scale bars in **E–H**: 25 μ m. The images of worms, sporocysts and eggs, were taken from representative specimens collected from the biological replicate “Experiment 7, tags 50 and 61”, “Experiment 11, tag 19 (panel **E**) and “Experiment 2, tag 6 (panel **G**)”, and “Experiment 1, tag 4”, respectively.

(**Figures 2E, G, Extended data Figure S5A, B³², and Movie 4⁴¹**), whereas within eggs the signal was mainly localised outside the larvae, but inside the eggshell (**Figures 2F, H**). Importantly, no autofluorescence signal was seen in control parasites (**Extended data Figures S4D, F, and S5C, D³²**).

Evident CRISPR-Cas9-induced deletions in exon 1 of *SULT-OR*

The CRISPR-Cas9 transfection experiments were performed on adult worms (3 biological replicates), mother sporocysts (2 biological replicates) and eggs (3 biological replicates). All replicates were performed by different experimentalists on different days as indicated in **Extended data Table S1³²**. DNA was extracted from the parasites four days after transfection, and a 262-bp PCR product spanning the gRNA region was amplified (**Figure 1C**) and sequenced on an Illumina MiSeq platform. The *SULT-OR*-specific PCR primers were designed in regions that are divergent between *SULT-OR* and the other paralogous genes (**Extended data Figure S3B, C³²**). With the assistance of the CRISPResso software^{34,35} we searched for mutations in the sequence reads by aligning reads to the reference amplicon. Remarkably, the percent of aligned reads that contained deletions was significantly higher

for CRISPR-Cas9-treated samples than for matched controls when we pooled all tested developmental stages (**Figure 3A** and **Extended data Table S1³²**; paired one-sided Wilcoxon test: $n=8$ biological replicates, $P=0.04$). In contrast, the percent of aligned reads with insertions or substitutions was not consistently higher in CRISPR-Cas9-treated samples than matched controls ($P=0.2$ for insertions and $P=0.9$ for substitutions; **Extended data Figure S6B, C³²**). Importantly, no evident differences were observed among the three types of controls employed in the experiments (**Extended data Table S1**). The apparent substitutions seen in both CRISPR-treated and control samples are likely due to sequencing errors, especially at the ends of the amplicon, since the two reads of a read-pair overlap in a 38-bp region in the centre of the amplicon, allowing CRISPResso to infer a higher-quality consensus sequence for that central region (**Figure 1C**).

Remarkably, a closer examination revealed that all three biological replicates of CRISPR-Cas9-treated adult worms had large deletions absent from control samples, extending from the predicted Cas9 cut site to about 60 bp upstream (**Figure 3B, C**). Considering the reads that contained a single internal deletion spanning the predicted Cas9 cut site, and no internal

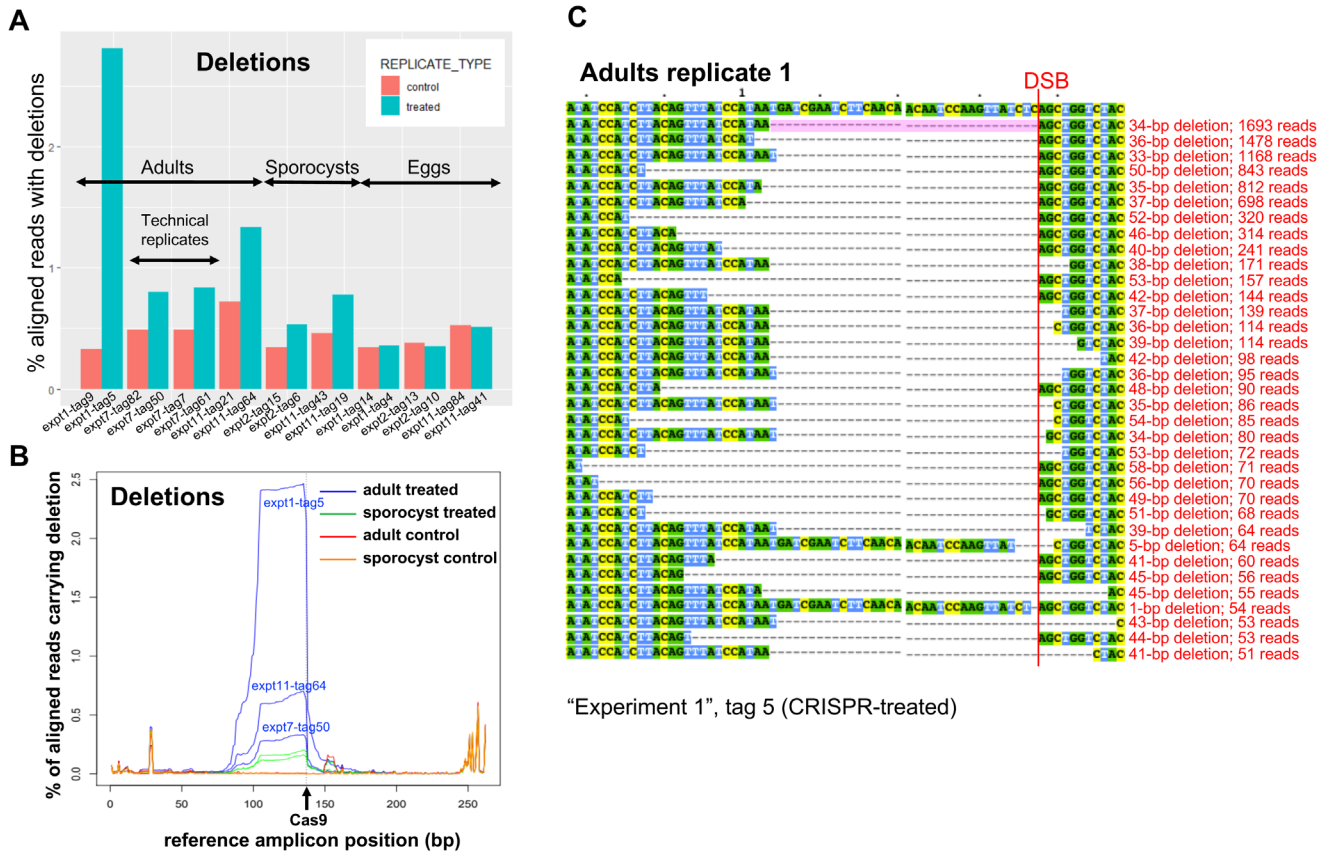


Figure 3. (A) Frequency of deletions in NGS sequencing data, identified with the assistance of CRISPResso in three biological replicates from adults, two from sporocysts, and three from eggs, as indicated. (B) CRISPR-induced deletions in adult worms and sporocysts. The positions of deletions found by CRISPResso in the reference amplicon are indicated, in three biological replicates of CRISPR-Cas9-treated adult samples (blue lines: experiment 1, tag 5; experiment 7, tag 50; experiment 11, tag 64) and matched adult control samples (red lines: experiment 1, tag 9; experiment 7, tag 82; experiment 11, tag 21), and in two biological replicates of CRISPR-Cas9-treated sporocysts (green lines: experiment 2, tag 6; experiment 11, tag 19) and matched sporocyst controls (orange lines: experiment 2, tag 15; experiment 11, tag 43). The black arrow shows the predicted Cas9 cut site. (C) Multi-sequence alignment of *SULT-OR* alleles with deletions found in CRISPR-Cas9-treated adult worms that are supported by $>=50$ reads and span the DSB site indicated with a red line, based on one of the treated adult replicates (experiment 1, tag 5). The common 34-bp deletion is highlighted in pale pink.

insertions, we found that 0.3-2.0% of aligned reads from CRISPR-Cas9-treated adult worms exhibited such deletions, compared to 0.0% of aligned reads from matched controls (Extended data Table S1³²).

Higher CRISPR-induced mutation rate in adults compared to sporocysts and eggs

Interestingly, up to 10 times more reads containing deletions spanning the predicted Cas9 cut site were detected in CRISPR-Cas9-treated adult worms (0.3-2.0% of aligned reads) compared to CRISPR-Cas9-treated sporocysts (0.1-0.2%; Extended data Table S1³²). In contrast, in eggs the rate of such deletions was not any higher than in matched controls (Extended data Table S1³²).

Deletions of the same size, and in the same position, were identified in CRISPR-Cas9-treated sporocysts and adults, being

absent from respective matched controls (Figure 3B). In addition, across different biological replicates of CRISPR-Cas9-treated adults and sporocysts, the most frequent deletion alleles (i.e. those for which we detected the most supporting reads) had roughly the same sizes and positions (Figure 3C and Extended data Figure S7³²). The most common deletion identified in all three adult biological replicates, and in one of the two sporocyst biological replicates, was 34 bp directly upstream of the predicted Cas9 cut site (spanning positions 104-137 in the reference amplicon). We observed rare deletions that were up to three times longer: that is, deletions that extended from the predicted Cas9 cut site to 102 bp upstream (to position 36 in the reference amplicon). Strikingly, none of these deletions were apparent in CRISPR-Cas9-treated eggs.

Almost all the deletions observed extended upstream from the predicted Cas9 cut site; rare deletions extending both

upstream and downstream of the cut site were identified but at relatively lower frequency, although often supported by 50 or more reads (**Extended data Figure S7³²**). In all biological replicates from adults, we did observe extremely low-frequency deletions, supported by few reads (<50 reads, not shown in **Extended data Figure S7³²**), extending from the predicted Cas9 cut site to 102 bp upstream (position 36 in the reference amplicon), and deletions spanning the cut site that extended as far as 79 bp downstream of the cut site (position 216 in the amplicon).

The percent of aligned reads carrying deletions that spanned the predicted Cas9 cut site did not differ between CRISPR-Cas9-treated eggs and control eggs. This suggested that in eggs either CRISPR-Cas9 did not introduce mutations in *SULT-OR* or they had occurred at an extremely low level. The presence of a recognition site for the restriction enzyme PvuII overlapping the predicted Cas9 cut site (**Figure 1B**) allowed us to develop a protocol to enrich for mutant alleles. Any CRISPR-Cas9-induced deletions that extended upstream from the Cas9 cut site would remove this PvuII recognition site, so by digesting the DNA from treated parasites with PvuII, we expected to enrich for CRISPR-Cas9-induced deletions. In

two out of three biological replicates of CRISPR-Cas9-treated egg samples, after PvuII treatment we were able to detect a slightly higher rate of deletions spanning the predicted Cas9 cut site, compared to in PvuII-treated control egg samples, i.e. an increase of at least 2-fold (**Extended data Table S1³²**), even though these deletions were still at very low frequency. This finding indicates that CRISPR-Cas was indeed active in eggs, although at very low levels.

Evidence for large deletions

Large CRISPR-induced deletions of >500 bp have been observed in the nematode *Strongyloides stercoralis*²⁰. In addition to the most common CRISPR-Cas9-induced deletions observed in *S. mansoni* that extended 34 bp upstream of the predicted Cas9 cut site (**Figure 3B**), we did observe low-frequency deletions (supported by few reads) extending from the predicted Cas9 cut site to 102 bp upstream (to position 36 in the reference amplicon) (**Figure 4** and **Extended data Figure S8³²**). We simulated reads carrying deletions of every possible length, extending upstream from the predicted Cas9 cut site, that is, a read carrying a deletion of 1-bp upstream of the Cas9 cut site, a read carrying a deletion of 2-bp upstream of the Cas9 cut site, reads with deletions of 3-bp, 4-bp, 5-bp, and so

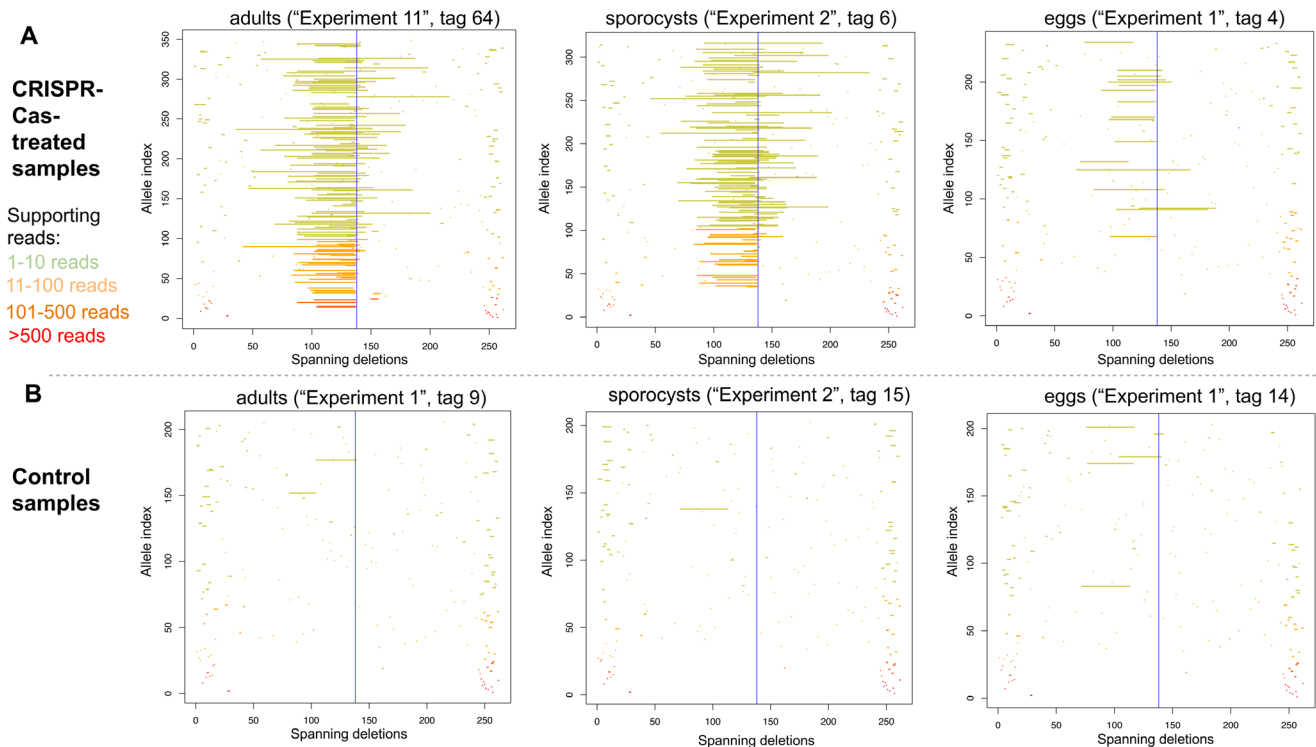


Figure 4. Deletion alleles seen in the *SULT-OR* gene in amplicon sequencing reads from treated (**A**) and control (**B**) adults (left), sporocysts (centre), and eggs (right), showing alleles that contain a single internal deletion and no internal insertions with respect to the reference amplicon. The y-axis shows deletion alleles sorted by the number of reads supporting them, with the alleles supported by the most reads at the bottom. Alleles supported by >500 reads in red, alleles supported by 101-500 reads in dark orange, alleles supported by 11-100 reads in pale green, and alleles supported by 1-10 reads in yellow. The x-axis shows the position of the deletion along the reference amplicon, with a blue vertical line at the predicted Cas9 cut site.

on. Using our parameter settings, CRISPResso detected the simulated deletions of sizes ranging from 1-bp up to 104-bp upstream of the predicted Cas9 cut site, but could not detect simulated deletions extending 105 bp or further upstream of the Cas9 cut site. This is presumably because, by default, CRISPResso requires that a read aligns with at least 60% identity to the reference amplicon, thus, discarding reads carrying simulated deletions spanning 40% (i.e. 105 bp) or more of our 262-bp reference amplicon. Given that in our real data (Figure 4 and Extended data Figure S8³²), we observed low-frequency deletions extending up to 102 bp upstream of the predicted Cas9 cut site, it is possible that in reality even longer deletions did also occur, but they would not have been detected, either because the reads were discarded by CRISPResso, or one or both PCR primer regions were deleted.

Deletions predicted to cause oxamniquine resistance

Relative to the *SULT-OR* amplicon, the start codon is located at position 103 and the predicted Cas9 cut site at position 137. In adult worms and sporocysts, the CRISPR-Cas9-induced deletions extended upstream from the predicted cut site into the first exon. The most common deletions extended 34 bases upstream, completely removing the first coding exon (barring a single a base) and shifting the reading frame of the entire coding region (Figure 1C and Extended data Figure S7³²). This would result in the preferential degradation of the mutant mRNAs, as previously suggested to explain the *ol* knockdown at the mRNA level observed in CRISPR-Cas9-treated eggs²¹. Moreover, any remaining frame-shifted SULT-OR protein is predicted to have lost its ability to convert OXA to its active drug form. Furthermore, even longer deletions upstream of the predicted Cas9 cut site were observed (Extended data Figure S7³²), which may extend into the *SULT-OR* promoter region given the 5'-UTR spans only 46 bp upstream of the first protein-coding codon, and hence may ablate the transcription of *SULT-OR*. The large CRISPR-Cas9-induced deletions, if they are homozygous, are predicted to cause resistance to OXA, either by producing frameshifts in the *SULT-OR* mRNA or by ablating *SULT-OR* transcription. However, when we analysed the expression levels of *SULT-OR* mRNA by qRT-PCR across preparations of whole parasites in CRISPR-Cas9-treated samples versus control adult worms, no differences were evident (not shown).

Extended data: Video files for 'Large CRISPR-Cas-induced deletions in the oxamniquine resistance locus of the human parasite *Schistosoma mansoni*'.

4 video files.

<https://doi.org/10.6084/m9.figshare.12631670.v141>

Discussion

Genome editing mediated by CRISPR-Cas has been recently applied to *S. mansoni* to knock out the egg-specific gene *omega-1* (*ol*)²¹. The CRISPR-Cas9 treatment of eggs by electroporation in the presence of the RNP complex, or egg transduction with lentivirus particles expressing Cas9 and the gRNA, induced a detectable knock-down both at the mRNA and protein levels and a clear phenotype of smaller

granulomas in mice exposed to CRISPR-Cas9-treated eggs. In the current study, we decided to employ CRISPR-Cas9 to target the *SULT-OR* sulfotransferase gene in *S. mansoni* with an RNP complex. Strikingly, we detected large deletions of ≥ 34 bp extending upstream of the predicted Cas9 cut site, whereas deletions extending downstream of the cut site were extremely rare. The tendency for deletions to be upstream of the predicted Cas9 cut site agrees with observations in mouse cell lines⁴². We identified deletions extending up to 102 bp upstream of the predicted Cas9 cut site, reaching the limit detectable with CRISPResso (104 bp upstream, using our own parameter settings), suggesting that even larger deletions may have been missed. Deletions of several hundred base pairs have been described in *Strongyloides*²⁰, *C. elegans*⁴³, and mammalian cell-lines^{42,44}. In addition, we characterised CRISPR-Cas9-induced mutations across three discrete developmental stages: adult worms, eggs, and *in vitro*-transformed sporocysts. The deletions spanning the predicted Cas9 cut site were most commonly detected in adult worms (0.3-2.0% of aligned reads), followed by sporocysts (0.1-0.2%), and extremely rare in eggs. Interestingly, no evidence for CRISPR-Cas9-induced insertions or substitutions in the *SULT-OR* gene was observed. An interesting question is whether the pattern of CRISPR-Cas9-induced mutations varies from gene-to-gene. When targeting the *ol* gene in the absence of donor molecule, where CRISPR-Cas9-induced mutations presumably occurred by non-homologous end joining (NHEJ)¹⁹, the overall rate of deletions detected in reads from CRISPR-Cas9-treated eggs was not higher than in control eggs²¹. This is consistent with an extremely low rate of NHEJ-mediated deletions in the *ol* gene in eggs, similar to what we described here for the genome editing of the *SULT-OR* gene in eggs. On the other hand, when the *ol* gene was targeted using CRISPR-Cas9 in the presence of a ssODN donor molecule, rare larger deletions spanning the predicted Cas9 cut site were detected in the CRISPR-Cas9-treated eggs compared to controls²¹. Since this effect was only observed in the presence of the donor molecule, it is tempting to speculate that those large deletions in the *ol* gene may have been related to the homology directed repair (HDR) mechanism involved in the knock-in of the donor molecule rather than driven by NHEJ⁴⁵. In addition, differences between protocols employed for *ol* and *SULT-OR* may have resulted in different spectra of CRISPR-Cas9-induced mutations: the CRISPR-Cas9-treated eggs sequenced in the *ol* study were transduced with lentivirus encoding a single-gRNA and Cas9 nuclease²¹, whereas we induced mutations in *SULT-OR* by electroporating the parasites with an *in vitro*-assembled RNP complex of Cas9 nuclease and a two-piece gRNA. Interestingly, in the liver fluke *Opisthorchis viverrini* electroporated in the presence of a plasmid encoding a single-gRNA and Cas9 nuclease, small deletions of up to ~10 bp and insertions of up to 2 bp were detected near the predicted Cas9 cut site in the granulin gene²².

Our data suggest that for *SULT-OR* the highest CRISPR efficiency was in adults, followed by sporocysts, and the lowest efficiency in eggs. For the latter we only found such deletions in <0.02% of aligned reads even after using PvuII to enrich

for mutant reads. Three possible non-mutually exclusive hypotheses may explain these differences. Firstly, electroporation of the RNP complex may be most efficient in adults and least efficient in eggs, possibly because the surface area:volume ratio of an adult worm is greater than that of a sporocyst or egg, and/or because the egg has a protective coating that makes it hard to penetrate⁴⁶. However, microporous and internal microchannels shown to be scattered across *Schistosoma* eggshells would allow the interchange of macromolecules with the host tissues⁴⁷. Relevant for us, the diameter of the smallest pores in *S. mansoni* eggs is 100 nm, and we have estimated the diameter of the RNP complex, assuming a globular shape, to be ~10 nm⁴⁸ indicating that the complex could have entered the egg through the pores. A second possibility is that some key NHEJ repair enzymes required for CRISPR have higher expression in adults than in sporocysts or eggs; according to RNAseq metadata²⁵ this is the case for *Smp_211060*, previously identified²¹ as a homolog of the Ku70/Ku80 genes that play a key role in NHEJ⁴⁹. Finally, CRISPR might be more efficient in inducing mutations in *SULT-OR* in adults than sporocysts or eggs, because *SULT-OR* is expressed more in the former developmental stage, making its chromatin more open and therefore more accessible to the CRISPR machinery^{19,50–52}.

To create a CRISPR-Cas9-mediated mutant of any schistosome gene in every cell of the animal, the germline cells need to be targeted and mutated by a germline transgenesis approach. So far, only two studies demonstrated germline transmission of exogenous DNA in schistosomes. An early study published in 2007⁵³ showed that a GFP-expressing plasmid was introduced into the miracidium germ cells by particle bombardment. Subsequently, the transfected miracidia infected snails, and resulting cercariae were employed to infect hamsters and obtain F1 transformed eggs. However, over a few generations the transformed parasites died and/or (as expected) the plasmid was diluted or lost. A few years later, germline transmission of integrated retroviral transgenes was demonstrated. Murine Leukemia Retrovirus (MLV) transgenes transduced the germ cells of eggs and were propagated through both the intrasnailed asexual developmental stages and intramammalian sexual developmental stages, reaching the F1 eggs^{16,17}. However, no germline transgenesis approach has yet been achieved using CRISPR-Cas in schistosomes. Ittiprasert *et al.* in 2019²¹ applied the CRISPR technology using a lentivirus expressing Cas9 and the gRNA, plus a donor, to introduce a 24-bp insertion (by HDR) into the *ol* gene in *S. mansoni* eggs. Intriguingly, although the expression of the *ol* gene was reduced by 81–83% after CRISPR-Cas9 treatment using the donor molecule, only ~4.5% of reads were identified by amplicon sequencing as mutated by indels (with <1% showing deletions) or substitutions, and only 0.19% of reads contained the 24-bp insertion. Proposed explanations for this discrepancy include a preferential penetration of CRISPR-Cas9 machinery (lentivirus and donor) in the envelope of the egg, where *ol* may be expressed⁴⁶, and/or the presence of large deletions that removed either one or both primer regions and so were not detected by amplicon sequencing (as seen in *Strongyloides*²⁰). Similarly, expression of the *Opisthorchis viverrini* granulin gene was reduced by >80% after CRISPR-Cas9 treatment of pooled adults in the absence of a donor, but only 1.3% of amplicon

sequencing reads contained indel mutations²². This apparent anomaly may be due to the predominant expression of the granulin gene in the *O. viverrini* tegument and gut, where electroporation of the gene editing plasmid may have been most efficient²². Furthermore, there may be variation in CRISPR-Cas9 efficiency between individual adults: taking adult *Opisthorchis* worms from hamsters that had been infected 60 days previously with CRISPR-treated newly encysted juveniles (NEJs), individual adults in which there was a greater knock-down at the mRNA level showed a far greater level of mutations upon amplicon sequencing, especially deletions and substitutions²². In this species, significant variation was seen in CRISPR-Cas9 efficiency between life stages. Using a plasmid encoding Cas9 and gRNA, a knock-down of >80% of granulin mRNA levels was achieved in adults and NEJs, but of <4% in metacercariae, possibly due to inefficient electroporation of the plasmid through the metacercarial cyst wall²².

In our study, while amplicon sequencing revealed reads carrying CRISPR-Cas9-induced mutations in *SULT-OR*, a knock-down of *SULT-OR* at the mRNA level was not evident, probably because the deletions occurred in only a small fraction of the adult cells that express *SULT-OR*. Single-cell sequencing data from adults shows *SULT-OR* is a marker of parenchymal cells¹⁰, while our confocal microscopy data suggest the Cas9-gRNA complex penetrated better into the adult tegument and intestine compared to parenchymal tissue. The same phenomenon was previously described in the liver fluke *Fasciola hepatica* when delivering fluorescently labelled molecules by electroporation^{54,55}, suggesting the flatworm intestine as the main point of entry when this delivery approach is employed. Furthermore, *SULT-OR* is also expressed at a low level in many other cell types in adults (**Extended data Figure S2B**³²). The large deletions spanning the predicted Cas9 cut site were found in 0.3–2.0% of aligned reads from CRISPR-treated adult worms, so our best estimate of the fraction of adult cells in which CRISPR worked is 0.3–2.0%. Since a pool of five adult worms were transfected with the RNP complex, the efficiency of CRISPR (and the amount of knock-down at the mRNA level) may have varied between worms, as well as between cells of an individual worm.

To conclude, more work is required to optimise CRISPR-Cas protocols to work best at different developmental stages and in particular tissues, and understand whether these differing protocols will result in different spectra of mutations⁴³ and degrees of mRNA knock-down. To do this, it may be critical to identify the mechanisms underlying CRISPR-Cas-induced mutations in schistosomes in each case (e.g. NHEJ, HDR or other mechanisms such as polymerase theta-mediated end-joining⁵⁶). Addressing these items would help the research community to achieve the holy grail of targeting the germ line and creating a stable knock-out or knock-in strain of any gene of interest.

Data availability

Underlying data

Large CRISPR-Cas induced deletions in the oxamniquine resistance locus of the human parasite *Schistosoma mansoni*,

Accession number: ERP 121238 <https://identifiers.org/ena.embl:ERP121238>

Open Science Framework: Large CRISPR-Cas-induced deletions in the oxamniquine resistance locus of the human parasite *Schistosoma mansoni*. <https://doi.org/10.17605/OSF.IO/DW3CN>³²

This project contains the following underlying data:

- qPCR_rawCts_exp2_Sankaranarayanan, Coghlan_etal_WOR.xls (raw Cts values)
- qPCR_rawCts_exp7_Sankaranarayanan, Coghlan_etal_WOR.xls (raw Cts values)
- Fig2A_Sankaranarayanan, Coghlan_etal_WOR.tif (original picture Figure 2, panel A)
- Fig2B-D_Sankaranarayanan, Coghlan_etal_WOR.tif (original picture Figure 2, panels B-D)
- Fig2E_Sankaranarayanan, Coghlan_etal_WOR.tif (original picture Figure 2, panel E)
- Fig2F_Sankaranarayanan, Coghlan_etal_WOR.tif (original picture Figure 2, panel F)
- Fig2G_Sankaranarayanan, Coghlan_etal_WOR.tif (original picture Figure 2, panel G)
- Fig2H_Sankaranarayanan, Coghlan_etal_WOR.tif (original picture Figure 2, panel H)
- FigS4A-C_Sankaranarayanan, Coghlan_etal_WOR.tif (original picture Figure S4, panel A-C)
- FigS4D_Sankaranarayanan, Coghlan_etal_WOR.tif (original picture Figure S4, panel D)
- FigS4E_Sankaranarayanan, Coghlan_etal_WOR.tif (original picture Figure S4, panel E)
- FigS4F_Sankaranarayanan, Coghlan_etal_WOR.tif (original picture Figure S4, panel F)
- FigS4G_Sankaranarayanan, Coghlan_etal_WOR.tif (original picture Figure S4, panel G)
- FigS5A_Sankaranarayanan, Coghlan_etal_WOR.tif (original picture Figure S5, panel A)
- FigS5B_Sankaranarayanan, Coghlan_etal_WOR.tif (original picture Figure S5, panel B)
- FigS5C_Sankaranarayanan, Coghlan_etal_WOR.tif (original picture Figure S5, panel C)
- FigS5D_Sankaranarayanan, Coghlan_etal_WOR.tif (original picture Figure S5, panel D)

Extended data

Open Science Framework: Large CRISPR-Cas-induced deletions in the oxamniquine resistance locus of the human parasite *Schistosoma mansoni*. <https://doi.org/10.17605/OSF.IO/Z45BG>³²

This project contains the following extended data:

- Sankaranarayanan, Coghlan_etal_WOR_extended_data_16Jul2020.docx (Word document containing legends for extended data)
- TableS1_Sankaranarayanan, Coghlan_etal_WOR.xlsx (Extended Data Table S1)
- TableS2_Sankaranarayanan, Coghlan_etal_WOR.xlsx (Extended Data Table S2)
- TableS3_Sankaranarayanan, Coghlan_etal_WOR.xlsx (Extended Data Table S3)
- FigS1_Sankaranarayanan, Coghlan_etal_WOR.pdf (Extended Data Figure S1)
- FigS2_Sankaranarayanan, Coghlan_etal_WOR.pdf (Extended Data Figure S2)
- FigS3_Sankaranarayanan, Coghlan_etal_WOR.pdf (Extended Data Figure S3)
- FigS4_Sankaranarayanan, Coghlan_etal_WOR.pdf (Extended Data Figure S4)
- FigS5_Sankaranarayanan, Coghlan_etal_WOR.pdf (Extended Data Figure S5)
- FigS6_Sankaranarayanan, Coghlan_etal_WOR.pdf (Extended Data Figure S6)
- FigS7_Sankaranarayanan, Coghlan_etal_WOR.pdf (Extended Data Figure S7)
- FigS8_Sankaranarayanan, Coghlan_etal_WOR.pdf (Extended Data Figure S8)

Data are available under the terms of the [Creative Commons Zero](https://creativecommons.org/licenses/by/4.0/) “No rights reserved” data waiver (CC0 1.0 Public domain dedication).

Figshare: Video files for ‘Large CRISPR-Cas-induced deletions in the oxamniquine resistance locus of the human parasite *Schistosoma mansoni*. <https://doi.org/10.6084/m9.figshare.12631670.v1>⁴¹

This project contains the following video files:

- 16031-V1-2-MovieS1_20Apr2020.mov

Movie 1. Serial optical sections of a *S. mansoni* male adult worm transfected with fluorescently labelled Cas9-gRNA (ATTO™ 550 signal in red), fixed and DAPI-stained (DAPI signal in aqua blue). Scale bar: 100 µm.

- 16031-V1-2-MovieS2_20Apr2020.mov

Movie 2. Serial optical sections of a *S. mansoni* male adult worm transfected with fluorescently labelled Cas9-gRNA (ATTO™ 550 signal in red), fixed and DAPI-stained (DAPI

signal in aqua blue). In these series of optical sections, the anterior end of the worm is observed. Scale bar: 100 μm .

- 16031-V1-2-MovieS3_20Apr2020.mov

Movie 3. Serial optical sections of a *S. mansoni* female adult worm transfected with fluorescently labelled Cas9-gRNA (ATTO™ 550 signal in red), fixed and DAPI-stained (DAPI signal in aqua blue). In these series of optical sections, the anterior end of the worm is observed. Scale bar: 100 μm .

- 16031-V1-2-MovieS4_20Apr2020.mov

Movie 4. Serial optical sections of a *S. mansoni* sporocyst transfected with fluorescently labelled Cas9-gRNA (ATTO™ 550 signal in red), fixed and DAPI-stained (DAPI signal in aqua blue). Scale bar: 25 μm .

Data are available under the terms of the [Creative Commons Attribution 4.0 International license](#) (CC-BY 4.0).

Author information

Patrick Driguez is currently affiliated with King Abdullah University of Science and Technology, Thuwal, Kingdom of Saudi Arabia.

Acknowledgments

We are grateful to colleagues at the Wellcome Sanger Institute; Simon Clare, Cordelia Brandt, Catherine McCarthy, Katherine Harcourt and Lisa Seymour for assistance and technical support with animal infections and maintenance of the *Schistosoma mansoni* life cycle; Carmen L. Diaz for sharing unpublished scRNAseq data from *in vitro*-sporocysts; Kate Rawlinson, Claire Cormie and David Goulding for technical assistance with the confocal microscopy; Steve Doyle, Marcus Lee, Katharina Boroviak, Sophie Adjalley and Andrew Bassett for informative discussions. We would like to thank James J. Collins III from The University of Texas Southwestern Medical Center, USA, for sharing scRNAseq data from adult worms.

References

- GBD 2015 Disease and Injury Incidence and Prevalence Collaborators: **Global, regional, and national incidence, prevalence, and years lived with disability for 310 diseases and injuries, 1990-2015: a systematic analysis for the Global Burden of Disease Study 2015.** *Lancet*. 2016; **388**(10053): 1545–1602. [PubMed Abstract](#) | [Publisher Full Text](#) | [Free Full Text](#)
- Gryseels B, Polman K, Clerinx J, *et al.*: **Human schistosomiasis.** *Lancet*. 2006; **368**(9541): 1106–1118. [PubMed Abstract](#) | [Publisher Full Text](#)
- Crellen T, Walker M, Lamberton PHL, *et al.*: **Reduced Efficacy of Praziquantel Against *Schistosoma mansoni* Is Associated With Multiple Rounds of Mass Drug Administration.** *Clin Infect Dis*. 2016; **63**(9): 1151–1159. [PubMed Abstract](#) | [Publisher Full Text](#) | [Free Full Text](#)
- Swain MT, Larkin DM, Caffrey CR, *et al.*: ***Schistosoma* comparative genomics: integrating genome structure, parasite biology and anthelmintic discovery.** *Trends Parasitol*. 2011; **27**(12): 555–64. [PubMed Abstract](#) | [Publisher Full Text](#) | [Free Full Text](#)
- Protasio AV, Tsai IJ, Babbage A, *et al.*: **A systematically improved high quality genome and transcriptome of the human blood fluke *Schistosoma mansoni*.** *PLoS Negl Trop Dis*. 2012; **6**(1): e1455. [PubMed Abstract](#) | [Publisher Full Text](#) | [Free Full Text](#)
- Stroehlein AJ, Korhonen PK, Chong TM, *et al.*: **High-quality *Schistosoma haematobium* genome achieved by single-molecule and long-range sequencing.** *Gigascience*. 2019; **8**(9): giz108. [PubMed Abstract](#) | [Publisher Full Text](#) | [Free Full Text](#)
- Luo F, Yin M, Mo X, *et al.*: **An improved genome assembly of the fluke *Schistosoma japonicum*.** *PLoS Negl Trop Dis*. 2019; **13**(8): e0007612. [PubMed Abstract](#) | [Publisher Full Text](#) | [Free Full Text](#)
- Wangwiwatsin A, Protasio AV, Wilson S, *et al.*: **Transcriptome of the parasitic flatworm *Schistosoma mansoni* during intra-mammalian development.** *bioRxiv*. [Publisher Full Text](#)
- Diaz Soria CL, Lee J, Chong T, *et al.*: **Single-cell atlas of the first intra-mammalian developmental stage of the human parasite *Schistosoma mansoni*.** *bioRxiv*. 2019; 754713. [Publisher Full Text](#)
- Wendt G, Zhao L, Chen R, *et al.*: **A single-cell RNAseq atlas of the pathogenic stage of *Schistosoma mansoni* identifies a key regulator of blood feeding.** *Microbiology*, *bioRxiv*. 2020; 69. [Publisher Full Text](#)
- Wang J, Paz C, Padalino G, *et al.*: **Large-scale RNAi screening uncovers new therapeutic targets in the human parasite *Schistosoma mansoni*.** *bioRxiv*. 2020; 2020.02.05.935833. [Publisher Full Text](#)
- Boutros M, Ahringer J: **The art and design of genetic screens: RNA interference.** *Nat Rev Genet*. 2008; **9**(7): 554–566. [PubMed Abstract](#) | [Publisher Full Text](#)
- Farboud B, Severson AF, Meyer BJ: **Strategies for Efficient Genome Editing Using CRISPR-Cas9.** *Genetics*. 2019; **211**(2): 431–457. [PubMed Abstract](#) | [Publisher Full Text](#) | [Free Full Text](#)
- Dickinson DJ, Goldstein B: **CRISPR-Based Methods for *Caenorhabditis elegans* Genome Engineering.** *Genetics*. 2016; **202**(3): 885–901. [PubMed Abstract](#) | [Publisher Full Text](#) | [Free Full Text](#)
- Suttiprapa S, Rinaldi G, Tsai IJ, *et al.*: **HIV-1 Integrates Widely throughout the Genome of the Human Blood Fluke *Schistosoma mansoni*.** *PLoS Pathog*. 2016; **12**(10): e1005931. [PubMed Abstract](#) | [Publisher Full Text](#) | [Free Full Text](#)
- Mann VH, Suttiprapa S, Skinner DE, *et al.*: **Pseudotyped murine leukemia virus for schistosome transgenesis: approaches, methods and perspectives.** *Transgenic Res*. 2014; **23**(3): 539–556. [PubMed Abstract](#) | [Publisher Full Text](#)
- Rinaldi G, Eckert SE, Tsai IJ, *et al.*: **Germline transgenesis and insertional mutagenesis in *Schistosoma mansoni* mediated by murine leukemia virus.** *PLoS Pathog*. 2012; **8**(7): e1002820. [PubMed Abstract](#) | [Publisher Full Text](#) | [Free Full Text](#)
- Hagen J, Young ND, Every AL, *et al.*: **Omega-1 knockdown in *Schistosoma mansoni* eggs by lentivirus transduction reduces granuloma size *in vivo*.** *Nat Commun*. 2014; **5**: 5375. [PubMed Abstract](#) | [Publisher Full Text](#) | [Free Full Text](#)
- Jiang F, Doudna JA: **CRISPR-Cas9 Structures and Mechanisms.** *Annu Rev Biophys*. 2017; **46**: 505–529. [PubMed Abstract](#) | [Publisher Full Text](#)
- Gang SS, Castelletto ML, Bryant AS, *et al.*: **Targeted mutagenesis in a human-parasitic nematode.** *PLoS Pathog*. 2017; **13**(10): e1006675. [PubMed Abstract](#) | [Publisher Full Text](#) | [Free Full Text](#)
- Ittiprasert W, Mann VH, Karinshak SE, *et al.*: **Programmed genome editing of the omega-1 ribonuclease of the blood fluke, *Schistosoma mansoni*.** *eLife*. 2019; **8**: e41337. [PubMed Abstract](#) | [Publisher Full Text](#) | [Free Full Text](#)
- Arunsan P, Ittiprasert W, Smout MJ, *et al.*: **Programmed knockout mutation of liver fluke granulin attenuates virulence of infection-induced hepatobiliary morbidity.** *eLife*. 2019; **8**: e41463. [PubMed Abstract](#) | [Publisher Full Text](#) | [Free Full Text](#)
- Valentim CLL, Cioli D, Chevalier FD, *et al.*: **Genetic and molecular basis of drug resistance and species-specific drug action in schistosome parasites.** *Science*. 2013; **342**(6164): 1385–1389. [PubMed Abstract](#) | [Publisher Full Text](#) | [Free Full Text](#)
- Pica-Mattoccia L, Dias LC, Moroni R, *et al.*: ***Schistosoma mansoni*: genetic complementation analysis shows that two independent hycanthone/oxamniquine-resistant strains are mutated in the same gene.** *Exp Parasitol*. 1993; **77**(4): 445–449. [PubMed Abstract](#) | [Publisher Full Text](#)

25. Lu Z, Zhang Y, Berriman M: **A web portal for gene expression across all life stages of *Schistosoma mansoni***. *bioRxiv*. 2018; 308213.
[PubMed Abstract](#) | [Publisher Full Text](#)
26. Mann VH, Morales ME, Rinaldi G, *et al.*: **Culture for genetic manipulation of developmental stages of *Schistosoma mansoni***. *Parasitology*. 2010; **137**(3): 451–462.
[PubMed Abstract](#) | [Publisher Full Text](#) | [Free Full Text](#)
27. Dalton JP, Day SR, Drew AC, *et al.*: **A method for the isolation of schistosome eggs and miracidia free of contaminating host tissues**. *Parasitology*. 1997; **115**(Pt 1): 29–32.
[PubMed Abstract](#) | [Publisher Full Text](#)
28. Rinaldi G, Morales ME, Alrefaei YN, *et al.*: **RNA interference targeting leucine aminopeptidase blocks hatching of *Schistosoma mansoni* eggs**. *Mol Biochem Parasitol*. 2009; **167**(2): 118–126.
[PubMed Abstract](#) | [Publisher Full Text](#) | [Free Full Text](#)
29. Kines KJ, Rinaldi G, Okatcha TI, *et al.*: **Electroporation facilitates introduction of reporter transgenes and virions into schistosome eggs**. *PLoS Negl Trop Dis*. 2010; **4**(2): e593.
[PubMed Abstract](#) | [Publisher Full Text](#) | [Free Full Text](#)
30. Rinaldi G, Okatcha TI, Popratiloff A, *et al.*: **Genetic manipulation of *Schistosoma haematobium*, the neglected schistosome**. *PLoS Negl Trop Dis*. 2011; **5**(10): e1348.
[PubMed Abstract](#) | [Publisher Full Text](#) | [Free Full Text](#)
31. Bolt BJ, Rodgers FH, Shafie M, *et al.*: **Using WormBase ParaSite: An Integrated Platform for Exploring Helminth Genomic Data**. *Methods Mol Biol*. 2018; **1757**: 471–491.
[PubMed Abstract](#) | [Publisher Full Text](#)
32. Rinaldi G: **Large CRISPR-Cas-induced deletions in the oxamniquine resistance locus of the human parasite *Schistosoma mansoni***. 2020.
<http://www.doi.org/10.17605/OSF.IO/Z45BG>
33. Bolger AM, Lohse M, Usadel B: **Trimmomatic: A Flexible Trimmer for Illumina Sequence Data**. *Bioinformatics*. 2014; **30**(15): 2114–2120.
[PubMed Abstract](#) | [Publisher Full Text](#) | [Free Full Text](#)
34. Canver MC, Haeussler M, Bauer DE, *et al.*: **Integrated Design, Execution, and Analysis of Arrayed and Pooled CRISPR Genome-Editing Experiments**. *Nat Protoc*. 2018; **13**(5): 946–986.
[PubMed Abstract](#) | [Publisher Full Text](#) | [Free Full Text](#)
35. Pinello L, Canver MC, Hoban MD, *et al.*: **Analyzing CRISPR Genome-Editing Experiments With CRISPResso**. *Nat Biotechnol*. 2016; **34**(7): 695–697.
[PubMed Abstract](#) | [Publisher Full Text](#) | [Free Full Text](#)
36. Ginzinger DG: **Gene Quantification Using Real-Time Quantitative PCR: An Emerging Technology Hits the Mainstream**. *Exp Hematol*. 2002; **30**(6): 503–512.
[PubMed Abstract](#) | [Publisher Full Text](#)
37. Livak KJ, Schmittgen TD: **Analysis of Relative Gene Expression Data Using Real-Time Quantitative PCR and the 2(-Delta Delta C_T) Method**. *Methods*. 2001; **25**(4): 402–408.
[PubMed Abstract](#) | [Publisher Full Text](#)
38. International Helminth Genomes Consortium: **Comparative genomics of the major parasitic worms**. *Nat Genet*. 2019; **51**(1): 163–174.
[PubMed Abstract](#) | [Publisher Full Text](#) | [Free Full Text](#)
39. Fincher CT, Wurtzel O, de Hoog T, *et al.*: **Cell type transcriptome atlas for the planarian *Schmidtea mediterranea***. *Science*. 2018; **360**(6391): eaaq1736.
[PubMed Abstract](#) | [Publisher Full Text](#) | [Free Full Text](#)
40. Zheng T, Hou Y, Zhang P, *et al.*: **Profiling Single-Guide RNA Specificity Reveals a Mismatch Sensitive Core Sequence**. *Sci Rep*. 2017; **7**: 40638.
[PubMed Abstract](#) | [Publisher Full Text](#) | [Free Full Text](#)
41. Sankaranarayanan G, Coghlan A, Driguez P, *et al.*: **Video files for 'Large CRISPR-Cas-induced deletions in the oxamniquine resistance locus of the human parasite *Schistosoma mansoni*'**. *Wellcome Open Research Media*. 2020.
<http://www.doi.org/10.6084/m9.figshare.12631670.v1>
42. Shin HY, Wang C, Lee HK, *et al.*: **CRISPR/Cas9 Targeting Events Cause Complex Deletions and Insertions at 17 Sites in the Mouse Genome**. *Nat Commun*. 2017; **8**: 15464.
[PubMed Abstract](#) | [Publisher Full Text](#) | [Free Full Text](#)
43. Chiu H, Schwartz HT, Antoshechkin I, *et al.*: **Transgene-free genome editing in *Caenorhabditis elegans* using CRISPR-Cas**. *Genetics*. 2013; **195**(3): 1167–1171.
[PubMed Abstract](#) | [Publisher Full Text](#) | [Free Full Text](#)
44. Kosicki M, Tomberg K, Bradley A: **Repair of Double-Strand Breaks Induced by CRISPR-Cas9 Leads to Large Deletions and Complex Rearrangements**. *Nat Biotechnol*. 2018; **36**(8): 765–771.
[PubMed Abstract](#) | [Publisher Full Text](#) | [Free Full Text](#)
45. Vu GTH, Cao HX, Fauser F, *et al.*: **Endogenous Sequence Patterns Predispose the Repair Modes of CRISPR/Cas9-induced DNA Double-Stranded Breaks in *Arabidopsis thaliana***. *Plant J*. 2017; **92**(1): 57–67.
[PubMed Abstract](#) | [Publisher Full Text](#)
46. Ashton PD, Harrop R, Shah B, *et al.*: **The Schistosome Egg: Development and Secretions**. *Parasitology*. 2001; **122**(Pt 3): 329–338.
[PubMed Abstract](#) | [Publisher Full Text](#)
47. Cao HM, Wang YF, Long S: **A Study of Ultrastructure of Egg Shell of *Schistosoma japonicum*. I. Transmission Electron Microscopic Observation of *S. japonicum* Egg**. *Ann Parasitol Hum Comp*. 1982; **57**(4): 345–352.
[PubMed Abstract](#) | [Publisher Full Text](#)
48. Erickson HP: **Size and Shape of Protein Molecules at the Nanometer Level Determined by Sedimentation, Gel Filtration, and Electron Microscopy**. *Biol Proced Online*. 2009; **11**: 32–51.
[PubMed Abstract](#) | [Publisher Full Text](#) | [Free Full Text](#)
49. Kragelund BB, Weterings E, Hartmann-Petersen R, *et al.*: **The Ku70/80 Ring in Non-Homologous End-Joining: Easy to Slip On, Hard to Remove**. *Front Biosci (Landmark Ed)*. 2016; **21**: 514–527.
[PubMed Abstract](#) | [Publisher Full Text](#)
50. Verkuijl SA, Rots MG: **The Influence of Eukaryotic Chromatin State on CRISPR-Cas9 Editing Efficiencies**. *Curr Opin Biotechnol*. 2019; **55**: 68–73.
[PubMed Abstract](#) | [Publisher Full Text](#)
51. Uusi-Mäkelä MIE, Barker HR, Bäuerlein CA, *et al.*: **Chromatin Accessibility Is Associated With CRISPR-Cas9 Efficiency in the Zebrafish (*Danio rerio*)**. *PLoS One*. 2018; **13**(4): e0196238.
[PubMed Abstract](#) | [Publisher Full Text](#) | [Free Full Text](#)
52. Jensen KT, Fløe L, Petersen TS, *et al.*: **Chromatin Accessibility and Guide Sequence Secondary Structure Affect CRISPR-Cas9 Gene Editing Efficiency**. *FEBS Lett*. 2017; **591**(13): 1892–1901.
[PubMed Abstract](#) | [Publisher Full Text](#)
53. Beckmann S, Wippersteg V, El-Bahay A, *et al.*: ***Schistosoma mansoni*: germ-line transformation approaches and actin-promoter analysis**. *Exp Parasitol*. 2007; **117**(3): 292–303.
[PubMed Abstract](#) | [Publisher Full Text](#)
54. Rinaldi G, Morales ME, Cancela M, *et al.*: **Development of Functional Genomic Tools in Trematodes: RNA Interference and Luciferase Reporter Gene Activity in *Fasciola hepatica***. *PLoS Negl Trop Dis*. 2008; **2**(7): e260.
[PubMed Abstract](#) | [Publisher Full Text](#) | [Free Full Text](#)
55. Dell'Oca N, Basika T, Corvo I, *et al.*: **RNA interference in *Fasciola hepatica* newly excysted juveniles: Long dsRNA induces more persistent silencing than siRNA**. *Mol Biochem Parasitol*. 2014; **197**(1–2): 28–35.
[PubMed Abstract](#) | [Publisher Full Text](#)
56. van Schendel R, Roerink SF, Portegijs V, *et al.*: **Polymerase θ is a key driver of genome evolution and of CRISPR/Cas9-mediated mutagenesis**. *Nat Commun*. 2015; **6**: 7394.
[PubMed Abstract](#) | [Publisher Full Text](#) | [Free Full Text](#)

Open Peer Review

Current Peer Review Status:    

Version 1

Reviewer Report 01 September 2020

<https://doi.org/10.21956/wellcomeopenres.17586.r39712>

© 2020 Skelly P. This is an open access peer review report distributed under the terms of the [Creative Commons Attribution License](#), which permits unrestricted use, distribution, and reproduction in any medium, provided the original work is properly cited.

 **Patrick Skelly** 

Molecular Helminthology Laboratory, Department of Infectious Disease and Global Health, Cummings School of Veterinary Medicine, Tufts University, North Grafton, MA, USA

This study by Sankaranarayanan & Coghlan *et al.* employed CRISPR-Cas9 to target for disruption the SULT-OR sulfotransferase gene in *Schistosoma mansoni* using electroporation to deliver a ribonucleoprotein (RNP) complex consisting of gRNA, tracrRNA and Cas9 protein. Mutations induced by this treatment were subsequently detected by high-throughput sequencing. The results provide independent confirmation that CRISPR/Cas delivery to *S. mansoni* can indeed induce mutations in these parasites, albeit (so far) at a low level. Three developmental stages were examined, and mutations were most commonly detected in adult worms (0.3-2.0% of aligned sequence reads), followed by sporocysts (0.1-0.2%), and were extremely rare in eggs. The work provides hope that ongoing research will permit researchers to use refined methods to target the germ line to create stable knock-out or knock-in strains of any schistosome gene of interest.

Some comments and questions:

Animal Procedures. Why were snails “moved into dark cupboards at 28°C when they start shedding cercariae” and is there a reference showing that this is helpful? Page 4: How was the water “conditioned”? (At least in my version) the “Welfare assessments....” sentence needs correcting.

Parasite Material. Useful, detailed methods are reported. So, for consistency, give specifics of the Percoll-sucrose solution.

CRISPR-Cas9 ribonucleoprotein complex assembly. Since we expect the gRNA and the nuclease to associate in a 1:1 ratio, why not mix these in equimolar amounts? How can the authors confirm that the gRNA and nuclease actually formed the RNP complex? Is there a way to determine how efficiently this occurred? Low efficiency might provide some explanation for the relatively low level of mutation detected here?

Bioinformatic analysis. Consider adding a reference to Phred Quality Scoring so that interested readers can make sense of the <23 score cut off. It may also be useful to define here “SNP” and “NHEJ”.

Results. CRISPR-Cas9 machinery.....The authors should report if ALL of the adults (males and females) yielded a similar staining pattern. In Figure 2A and Movie 1, surface staining is not uniform along the length of the worm; did all males exhibit such staining in a similar region and to a similar extent (and in all replicates)? Does any of the RNP staining co-localize with DAPI-stained nuclei? If yes, point examples out. If not, how well is the nuclear localization signal working?

Discussion. It is reported that “no evidence for CRISPR-Cas9-induced insertions or substitutions in the SULT-OR gene was observed.” For context, it would be useful to know how this equates (if possible, under comparable experimental conditions) with work in *Strongyloides*, *C. elegans*, and mammalian cell-lines.

I disagree that because mutations were detected in 2% of aligned reads, this necessarily means that ~2% of cells were impacted.

The control data shown in e.g. Figure 3A – were they derived from the mock treated worms or from worms treated with Cas9 only or from those treated with gRNA only? Or were data from all controls combined?

Report how the tree shown in Figure S1A was generated. What does “PRJEA36577” etc. refer to in the figure? What is the value of showing anything outside of the area bounded by the red dashed line?

Is the work clearly and accurately presented and does it cite the current literature?

Yes

Is the study design appropriate and is the work technically sound?

Yes

Are sufficient details of methods and analysis provided to allow replication by others?

Yes

If applicable, is the statistical analysis and its interpretation appropriate?

Yes

Are all the source data underlying the results available to ensure full reproducibility?

Yes

Are the conclusions drawn adequately supported by the results?

Yes

Competing Interests: No competing interests were disclosed.

Reviewer Expertise: Molecular parasitology.

I confirm that I have read this submission and believe that I have an appropriate level of expertise to confirm that it is of an acceptable scientific standard.

Reviewer Report 24 August 2020

<https://doi.org/10.21956/wellcomeopenres.17586.r39705>

© 2020 Pawlowic M. This is an open access peer review report distributed under the terms of the [Creative Commons Attribution License](#), which permits unrestricted use, distribution, and reproduction in any medium, provided the original work is properly cited.



Mattie Pawlowic 

Biological Chemistry and Drug Discovery, Wellcome Centre for Anti-Infectives Research, University of Dundee, Dundee, UK

Sankaranarayanan and colleagues report their work to mutate *Schistosoma mansoni* SULT-OR, a gene related to oxamniquine resistance, using transfection of ribonucleoprotein (RNP) complex to induce CRISPR/Cas9 double-stranded breaks. They use this approach on worm adults, sporocysts, and eggs, and deep sequence the resulting parasites to determine which mutations are present. This represents a new approach for genetic modification of *Schistosoma*.

The authors find that adult and sporocysts (not eggs) take up fluorescently labelled RNPs. These bind non-specifically on the surface of adult worms and also concentrate in the gut. In the future, the authors should visualise what uptake may occur in adult worms without electroporation, as it appears a significant amount of uptake may be due to feeding. It is curious that the Cas9, which contains a nuclear localisation sequence, does not localise the RNP complex to the nucleus of worm cells. It could be that the 4-hour time frame is too short to observe this, or it could be that lack of nuclear localisation may explain the low editing efficiency.

After 4 days of culture, the authors extracted DNA from transfected parasites, PCR amplified the region of interest, and deep sequenced to identify mutations. I understand that a larger PCR fragment is required to identify deletions, however the authors designed the ends of the PCR products to overlap at the Cas9 cut site. This led to difficulties in identifying true mutations vs sequencing errors at the cut site. Therefore, I think indels may be under-reported as they were not well captured.

The authors find that deletions are the most common mutations the occur at the SULT-OR locus. I disagree that deletions in the range of 24-102 bp should be called "large". Consistent with use of CRISPR in other systems, deletions occur upstream of the cut site. Although adult worms took up RNPs the best, the mutation rate was found to be only <2%. This is likely due to the RNPs not transfecting every cell in the adult worm.

Despite SULT-OR being at its highest expression levels in adult worms, mutation rates were too low to see a impact on SULT-OR expression levels.

Overall this work reports new methods for genetic modification of *Schistosoma mansoni*. While the

efficiency is low, further optimisation makes this approach promising.

Is the work clearly and accurately presented and does it cite the current literature?

Yes

Is the study design appropriate and is the work technically sound?

Yes

Are sufficient details of methods and analysis provided to allow replication by others?

Yes

If applicable, is the statistical analysis and its interpretation appropriate?

Yes

Are all the source data underlying the results available to ensure full reproducibility?

Yes

Are the conclusions drawn adequately supported by the results?

Yes

Competing Interests: No competing interests were disclosed.

Reviewer Expertise: Parasite genetics and biochemistry, Cryptosporidium.

I confirm that I have read this submission and believe that I have an appropriate level of expertise to confirm that it is of an acceptable scientific standard.

Reviewer Report 04 August 2020

<https://doi.org/10.21956/wellcomeopenres.17586.r39711>

© 2020 Jurberg A. This is an open access peer review report distributed under the terms of the [Creative Commons Attribution License](#), which permits unrestricted use, distribution, and reproduction in any medium, provided the original work is properly cited.



Arnon Jurberg

Oswaldo Cruz Foundation, Rio de Janeiro, Brazil

The work by Sankaranarayanan & Coghlan *et al.* sought to deploy CRISPR/Cas9 by electroporation at distinct developmental stages of schistosomes (more specifically, eggs, sporocysts and adult worms). A successful implementation of this technique in schistosomes will open up numerous possibilities for the study of gene function in these flatworms and is likely to revolutionize the field in the same manner as gene knockout by homologous recombination in mice and rats.

The paper is well written and provided a detailed description of their methods and findings. The figures are well conceived and the paper is likely to provide grounds for others to come, although

CRISPR efficiency rate was below 5%.

1. Considering the low editing efficiency, did the authors evaluate the activity of other gRNAs against *SULT-OR*?
2. It also caught my attention the apparent lack of nuclear staining for fluorescently labelled Cas9-gRNA. Did the authors address this?
3. It was also unclear to me whether the staining pattern between adult males and females were similar, and I would like to suggest the addition of further details. An alternative approach that can assist in achieving greater CRISPR efficiencies in schistosomes is the use of microinjection (perhaps in the ovary of females).
4. Once mutations in the target gene are predicted to induce oxamniquine resistance, did the authors evaluate whether incubation of electroporated parasites with this drug could improve CRISPR efficiency?

Is the work clearly and accurately presented and does it cite the current literature?

Yes

Is the study design appropriate and is the work technically sound?

Yes

Are sufficient details of methods and analysis provided to allow replication by others?

Yes

If applicable, is the statistical analysis and its interpretation appropriate?

Yes

Are all the source data underlying the results available to ensure full reproducibility?

Yes

Are the conclusions drawn adequately supported by the results?

Yes

Competing Interests: No competing interests were disclosed.

Reviewer Expertise: Developmental biology, molecular biology and gene editing, cell biology.

I confirm that I have read this submission and believe that I have an appropriate level of expertise to confirm that it is of an acceptable scientific standard.

Reviewer Report 30 July 2020

<https://doi.org/10.21956/wellcomeopenres.17586.r39710>

© 2020 LoVerde P. This is an open access peer review report distributed under the terms of the [Creative Commons Attribution License](#), which permits unrestricted use, distribution, and reproduction in any medium, provided the original work is properly cited.



Phillip LoVerde 

Department of Biochemistry and Structural Biology, University of Texas Health Science Center at San Antonio, San Antonio, TX, USA

Schistosomiasis remains a serious global health problem. The toolbox available to scientists continues to improve. The ability to manipulate genes is a key technique to the continued success of the field to address questions of biology, host-parasite interactions, vaccines, drugs and diagnostics among others. The manuscript by the Wellcome Sanger Group is a welcome addition as it provides very detailed methods, state of the art approach and detailed analysis of the results. In fact, it provides a roadmap for others to follow. This is in spite of the fact they were not successful in producing a drug resistant transgenic strain. Clearly part of the reason was that only somatic cells were affected by the CRISPR-Cas 9 construct. They recognize that affecting germ line cells will likely make a difference. Another plausible explanation is that the cells in which CRISPR-Cas9 did induce mutations represented a small fraction of the cells expressing SmSULT-OR. They also acknowledge that the resistance trait is double recessive inferring that both alleles must be interrupted. I may have missed it but did not see where they attempted to demonstrate that both alleles of SmSULT-OR were interrupted.

The manuscript is well-written and follows a logical progression with well-designed experiments. Suggest use the term intramolluscan instead of intrasnaill. An issue out of their control is the difficulty in navigating the Extended data Figures and Tables. However, all the data is available to the reader.

Is the work clearly and accurately presented and does it cite the current literature?

Yes

Is the study design appropriate and is the work technically sound?

Yes

Are sufficient details of methods and analysis provided to allow replication by others?

Yes

If applicable, is the statistical analysis and its interpretation appropriate?

Yes

Are all the source data underlying the results available to ensure full reproducibility?

Yes

Are the conclusions drawn adequately supported by the results?

Yes

Competing Interests: No competing interests were disclosed.

Reviewer Expertise: Schistosomiasis host-parasite interactions involving molecular, immunological and genetic approaches. Drug Discovery.

I confirm that I have read this submission and believe that I have an appropriate level of expertise to confirm that it is of an acceptable scientific standard.
